

# High piezoelectric properties of BaTiO<sub>3</sub>–xLiF ceramics sintered at low temperatures

Wei-Gang Yang, Bo-Ping Zhang\*, Nan Ma, Lei Zhao

*School of Materials Science and Engineering, University of Science and Technology Beijing, Beijing 100083, China*

Received 12 July 2011; received in revised form 27 October 2011; accepted 29 October 2011

Available online 3 December 2011

## Abstract

BaTiO<sub>3</sub>–xLiF ceramics were prepared by a conventional sintering method using BaTiO<sub>3</sub> powder about 100 nm in diameter. The effects of LiF content (*x*) and sintering temperature on density, crystalline structure and electrical properties were investigated. A phase transition from tetragonal to orthorhombic symmetry appeared as sintering temperatures were raised from 1100 °C to 1200 °C or as LiF was added from 0 mol% to 3 mol%. BaTiO<sub>3</sub>–6 mol% LiF ceramic sintered at 1000 °C exhibited a high relative density of 95.5%, which was comparable to that for pure BaTiO<sub>3</sub> sintered at 1250 °C. BaTiO<sub>3</sub>–4 mol% LiF ceramic sintered at 1100 °C exhibited excellent properties with a piezoelectric constant  $d_{33} = 270$  pC/N and a planar electromechanical coupling coefficient  $k_p = 45\%$ , because it is close to the phase transition point in addition to high density.

© 2011 Elsevier Ltd. All rights reserved.

**Keywords:** B. Grain size; C. Dielectric properties; C. Piezoelectric properties; D. BaTiO<sub>3</sub> and titanates; Low temperature sintering

## 1. Introduction

Lead-free piezoceramics are urgently needed to replace lead-based piezoceramics as a result of growing environmental concerns. Barium titanate (BaTiO<sub>3</sub>) is the first practically applied piezoceramics. Although BaTiO<sub>3</sub> ceramics had been reported to have a moderate  $d_{33}$  of 190 pC/N for several decades, the surprising high  $d_{33}$  values (350 pC/N, 460 pC/N, 788 pC/N) have been obtained recently by microwave sintering, two-step sintering, and template grain growth.<sup>1–3</sup> Unfortunately, these preparation methods are not suitable for mass production due to high cost or complex processes. Therefore, obtaining high piezoelectric properties of BaTiO<sub>3</sub> ceramics by traditional processes has attracted much attention. However, the ideal densification temperature of BaTiO<sub>3</sub> ceramics is as high as 1300 °C,<sup>4</sup> which also impedes the application of BaTiO<sub>3</sub> ceramics. Meanwhile, its grains are apt to grow up at a high sintering temperature. It is well known that finer grain sizes are favorable to obtain high-performance BaTiO<sub>3</sub> ceramics because of smaller domain sizes. Therefore, reducing sintering temperature is necessary for the fabrication and practical application of high performance BaTiO<sub>3</sub> piezoelectric ceramics. Several promising approaches

such as adding sintering aids, using chemical processing and reducing the particle size of the starting materials, have been explored.<sup>5</sup> Among them, adding sintering aids is a simple, effective and easily controllable method. Caballero et al.<sup>6</sup> reported that ZnO-doped BaTiO<sub>3</sub> ceramics sintered at 1250 °C showed a high relative density of 99% and a permittivity value close to 3000. LiF-containing additives are very effective in lowering the sintering temperature of BaTiO<sub>3</sub>. Naghib-Zadeh et al.<sup>7</sup> found that the relative density of BaTiO<sub>3</sub> ceramic sintered at 900 °C is more than 98% by adding 2 wt% LiF–SrCO<sub>3</sub>. However, little attention has been paid to the piezoelectric properties of BaTiO<sub>3</sub> ceramic other than its dielectric properties. The piezoelectric properties of BaTiO<sub>3</sub> ceramics are dependent not only on density but also grain size, impurities and structural defects.<sup>8</sup> To obtain high piezoelectric BaTiO<sub>3</sub> ceramics at a low sintering temperature, the LiF content and sintering temperature need to be optimized. In the present study, the density, phase structure and electrical properties of BaTiO<sub>3</sub>–xLiF ceramics were investigated with a special emphasis on the effects of LiF content (*x*) and sintering temperature.

## 2. Experimental procedures

Barium titanate (BaTiO<sub>3</sub>, 99%, 100 nm) and lithium fluoride (LiF, 99%) were used as raw materials. These powders

\* Corresponding author. Tel.: +86 10 62334195.

E-mail address: [bpzhang@ustb.edu.cn](mailto:bpzhang@ustb.edu.cn) (B.-P. Zhang).

were weighed according to the composition of  $\text{BaTiO}_3\text{-}x\text{LiF}$  ( $x=0\text{--}6\text{ mol\%}$ ). The mixture was milled by  $\text{ZrO}_2$  balls in an ethanol solution. After ball milling for 2 h, the slurry was dried at  $80^\circ\text{C}$ . The dry powders were then compacted to disks of 10 mm in diameter and 1.5 mm in thickness at 80 MPa using 2 wt% polyvinyl alcohol (PVA) as a binder, following which the disks were heated to  $600^\circ\text{C}$  at  $5^\circ\text{C}/\text{min}$  and held at  $600^\circ\text{C}$  for 1 h, thereby removing the binder. The samples were cooled to room temperature and then the temperature was raised directly to sintering temperature ( $1000\text{--}1250^\circ\text{C}$ ) at  $10^\circ\text{C}/\text{min}$  and held for 2 h. The specimens were coated with silver paint on their upper and bottom surfaces and fired at  $550^\circ\text{C}$  for 30 min for electrical measurement. The coated samples were poled under a dc field of  $1.5\text{--}3\text{ kV}/\text{mm}$  at room temperature for 30 min in a silicone oil bath. The density of the samples was determined by accurately measuring their mass, diameter and thickness. The crystal structure was studied using XRD with a Cu  $K\alpha$  radiation ( $\lambda = 1.5416\text{ \AA}$ ) filtered through a Ni foil (Rigaku; RAD-B system, Tokyo, Japan). The microstructure of the sintered samples was observed by scanning electron microscope (SEM, ZEISS-EVO18, Germany). The piezoelectric properties were measured using a quasi-static piezoelectric coefficient  $d_{33}$  testing meter (ZJ-3A, Institute of Acoustics, Chinese Academy of Sciences, Beijing, China). The planar electromechanical coupling coefficient  $k_p$  was determined by resonance–antiresonance method using an Agilent 4294A precision impedance analyzer (Hewlett-Packard, Palo Alto, CA). The dielectric properties were measured using an Agilent 4294A precision impedance analyzer (Hewlett-Packard, Palo Alto, CA) from 100 Hz to 1 MHz. The temperature dependence of the dielectric properties was examined using a programmable furnace with an LCR analyzer (TH2828S) at 1 kHz in the temperature range of  $13\text{--}150^\circ\text{C}$ . Ferroelectric hysteresis loops were measured at 100 Hz using a ferroelectric tester (RT6000HVA, Radiant Technologies, Inc., Albuquerque, NM).

### 3. Results and discussion

#### 3.1. Densification sintering

Fig. 1 shows the temperature dependence of relative densities for the  $\text{BaTiO}_3\text{-}x\text{LiF}$  ( $x=0\text{--}6\text{ mol\%}$ ) ceramics. Pure  $\text{BaTiO}_3$  sintered at  $1100^\circ\text{C}$  has a relative density of 83.4%, which reaches about 90% as the temperature is increased to  $1200^\circ\text{C}$  and peaks at approximately 95% at a sintering temperature of  $1250^\circ\text{C}$ . The relative density of  $\text{BaTiO}_3$  ceramics is greatly improved by introducing LiF. Adding only 3 mol% LiF into  $\text{BaTiO}_3$  sintered at  $1125^\circ\text{C}$  yields a relative density of over 90%, which is comparable to that of pure  $\text{BaTiO}_3$  sintered at  $1200^\circ\text{C}$ . The enhancement of the relative density becomes more remarkable as the LiF is increased. A sample with the relative density of 95.5% can be obtained by doping 6 mol% LiF at a sintering temperature of  $1000^\circ\text{C}$ , but the sintering temperature needs to be  $1250^\circ\text{C}$  to obtain the same relative density in pure  $\text{BaTiO}_3$  ceramics. The results suggest that introducing LiF into  $\text{BaTiO}_3$  ceramics can significantly enhance the densification of the ceramics by liquid phase sintering since the melting point of LiF is as low as

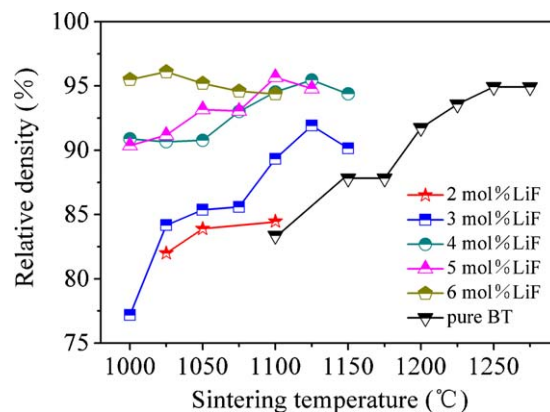


Fig. 1. Relationship of the relative density and sintering temperature for  $\text{BaTiO}_3\text{-}x\text{LiF}$  ceramics.

$846^\circ\text{C}$ .<sup>9</sup> Nevertheless, further raising the sintering temperature prejudices the densification of all LiF-added compositions, as a result of the evaporation of the LiF.<sup>9,10</sup> Akishige et al.<sup>10</sup> found that  $\text{F}^-$  evaporates in the range of  $740\text{--}1130^\circ\text{C}$  in 10% KF-doped  $\text{BaTiO}_3$  ceramics, based on TGA results. Marder et al.<sup>9</sup> reported that 1 wt% LiF doped  $\text{Y}_2\text{O}_3$  ceramics sintered at  $700^\circ\text{C}$  obtained the highest density, while the density decreased as the sintering temperature was raised to  $900^\circ\text{C}$ , as a result of the evaporation of LiF at high temperature.

Fig. 2 shows the optimal sintering temperature of the  $\text{BaTiO}_3\text{-}x\text{LiF}$  ( $x=0\text{--}6\text{ mol\%}$ ) ceramics with maximum density. Because of the high sintering activity of 100 nm  $\text{BaTiO}_3$  powder, the optimal sintering temperature for pure  $\text{BaTiO}_3$  is  $1250^\circ\text{C}$ , which is lower than the  $1300^\circ\text{C}$  which is usually necessary for fabricating dense  $\text{BaTiO}_3$  ceramics.<sup>4</sup> With the increase of  $x$  from 3 mol% to 6 mol%, the optimal sintering temperature is reduced from  $1125^\circ\text{C}$  to  $1025^\circ\text{C}$ . The optimal sintering temperature for  $\text{BaTiO}_3\text{-}6\text{ mol\% LiF}$  ceramic is reduced by  $225^\circ\text{C}$  as compared with that ( $1250^\circ\text{C}$ ) for pure  $\text{BaTiO}_3$ .

#### 3.2. Microstructure and phase structure

Fig. 3 shows the SEM images of the thermally etched surface of  $\text{BaTiO}_3\text{-}x\text{LiF}$  ceramics. All samples show clear grain boundaries. The grain sizes of pure  $\text{BaTiO}_3$  sintered at  $1100^\circ\text{C}$

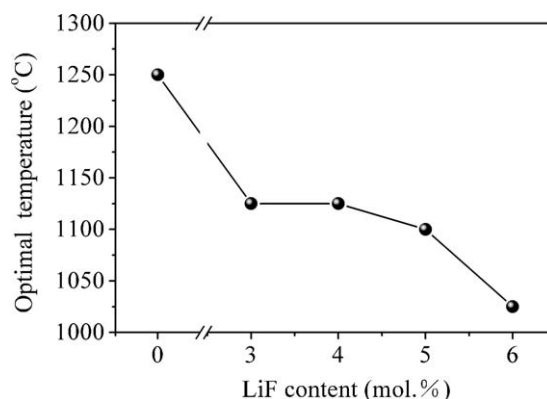


Fig. 2. Optimal sintering temperature of  $\text{BaTiO}_3\text{-}x\text{LiF}$  ceramics as a function of LiF content.

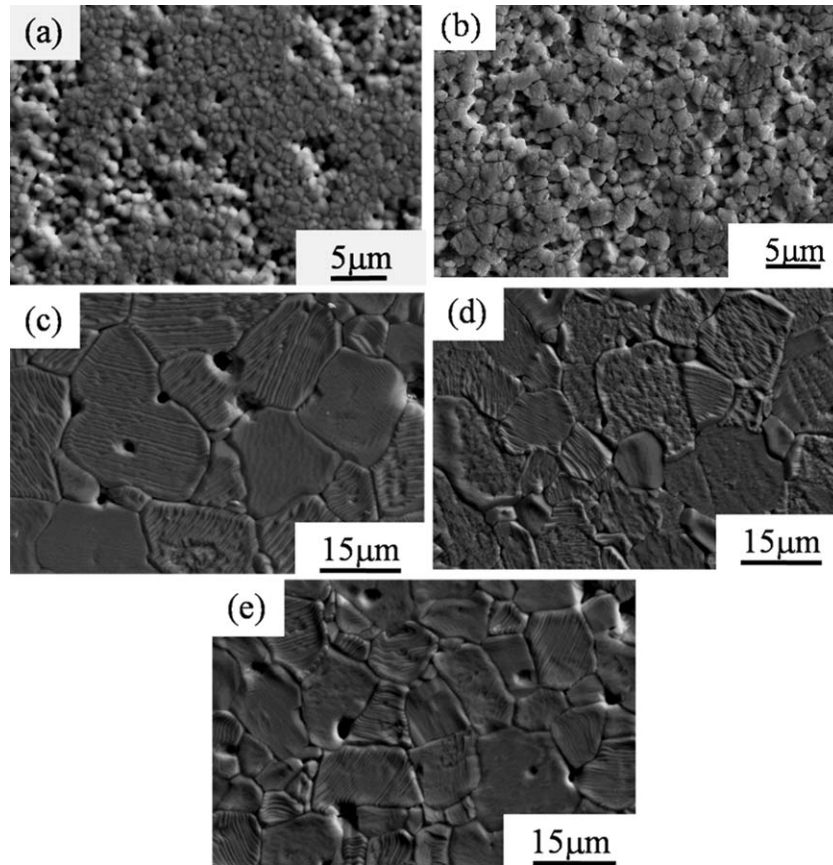


Fig. 3. SEM images of thermally etched surface of  $\text{BaTiO}_3\text{-}x\text{LiF}$  ceramics sintered at  $1100^\circ\text{C}$  (a, c–e) and at  $1200^\circ\text{C}$  (b). (a and b)  $x=0$  mol%; (c)  $x=4$  mol%; (d)  $x=5$  mol%; (e)  $x=6$  mol%.

and  $1200^\circ\text{C}$  are about  $0.85\text{ }\mu\text{m}$  and  $2.5\text{ }\mu\text{m}$ , respectively, while the grains grow to  $11\text{--}22\text{ }\mu\text{m}$  in the specimens to which LiF has been added. The reason is that liquid phase sintering greatly promotes grain growth.

Fig. 4(a) shows X-ray diffraction patterns of  $\text{BaTiO}_3\text{-}x\text{LiF}$  ceramics ( $x=0\text{--}6$  mol%) sintered at  $1100^\circ\text{C}$  and pure  $\text{BaTiO}_3$  ceramics sintered at  $1200^\circ\text{C}$ . The standard diffraction peaks cited from the tetragonal  $\text{BaTiO}_3$  (PDF#05-0626) and the orthorhombic one (PDF#81-2200) are indicated by vertical lines for comparison, whose ratios of two diffraction peaks around  $45^\circ$  are obviously different as shown in the enlarged XRD patterns of angles ranging from  $44^\circ$  to  $46^\circ$  in Fig. 4(b). The former ratio of (200) to (002) is greater than 1, while the later ratio of (200) to (002) is less than 1. All the samples exhibit a pure perovskite structure without any trace of impurity phase. The diffraction peaks for the pure  $\text{BaTiO}_3$  sintered at  $1100^\circ\text{C}$  correspond well with those of the PDF#05-0626, while those for the counterparts sintered at  $1200^\circ\text{C}$  and the LiF-added samples sintered at  $1100^\circ\text{C}$  correspond well with those of the PDF#81-2200, respectively. This result suggests that the crystallographic structure changes from tetragonal to orthorhombic symmetry by raising the sintering temperature from  $1100^\circ\text{C}$  to  $1200^\circ\text{C}$  or by adding LiF. On the other hand, when the LiF content varies from 0 mol% to 6 mol%, the (0 2 2) peak near  $45^\circ$  tends clearly toward lower diffraction angles, as a result of the enlargement of lattices, according to Bragg's equation ( $2d \sin \theta = \lambda$ ), because

of the substitutions of  $\text{Li}^+$  ( $r=0.76\text{ }\text{\AA}$ ) for  $\text{Ti}^{4+}$  ( $r=0.61\text{ }\text{\AA}$ ) in B site.<sup>11,12</sup>

### 3.3. Electrical properties

Fig. 5 shows the piezoelectric constant  $d_{33}$ , the planar electromechanical coupling coefficient  $k_p$  (a) and the grain size (b)

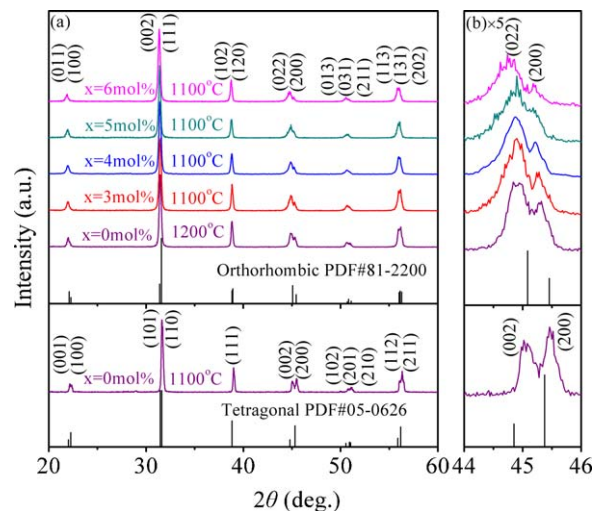


Fig. 4. X-ray diffraction patterns between the  $2\theta$  range of  $20\text{--}60^\circ$  (a) and  $44\text{--}46^\circ$  (b) for  $\text{BaTiO}_3\text{-}x\text{LiF}$  ceramics.



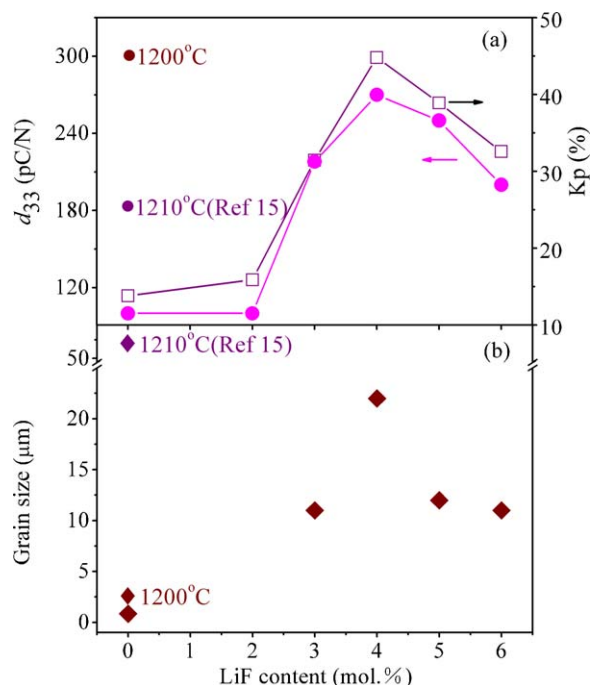


Fig. 5. The  $d_{33}$  and  $k_p$  (a) and grain size (b) for the BaTiO<sub>3</sub>-xLiF ceramics as a function of LiF content.

for the BaTiO<sub>3</sub>-xLiF ceramics sintered at 1100 °C as a function of LiF content. The  $d_{33}$  and grain size of pure BaTiO<sub>3</sub> sintered at 1200 °C are also shown for comparison. The pure BaTiO<sub>3</sub> sintered at 1200 °C with a grain size of 2.5 μm shows a high  $d_{33}$  value (300 pC/N), while the counterpart sintered at 1100 °C with a grain size of 0.85 μm exhibits a considerably low  $d_{33}$  value (100 pC/N) because of its low density (83.37%). The 4 mol% LiF added sample with a grain size of 22 μm exhibits a maximum  $d_{33}$  = 270 pC/N as the sintering was performed at 1100 °C. Fine grain size favors a high  $d_{33}$ , so the BaTiO<sub>3</sub> sample sintered at 1200 °C has a grain size of about 2.5 μm and shows a  $d_{33}$  = 300 pC/N which is much higher than 193 pC/N<sup>13</sup> for the sample with a grain size of >50 μm. Some previous reports<sup>1,4</sup> have also demonstrated that smaller grains tend to have smaller domain sizes and higher  $d_{33}$ , since the domain walls with small areas will respond more actively to external electrical or stress signals. The BaTiO<sub>3</sub>-4 mol% LiF ceramics with the biggest grain size (22 μm) show  $d_{33}$  value (270 pC/N), which is higher than the  $d_{33}$  values (218 pC/N, 250 pC/N, 200 pC/N) for counterparts obtained with smaller grain sizes. As mentioned above, the higher  $d_{33}$  value corresponds to the finer grain size, but this cannot explain the fact that the  $d_{33}$  value for BaTiO<sub>3</sub>-4 mol% LiF ceramics is higher than those for counterparts with smaller grain sizes. The lower  $d_{33}$  value (218 pC/N) in the 3 mol% LiF added sample is attributable to the relative density being less than 90%. The samples with 5–6 mol% LiF show smaller grain sizes (12, 11 μm) and similar densities as compared with that of the BaTiO<sub>3</sub>-4 mol% LiF, but their  $d_{33}$  values (250, 200 pC/N, respectively) are lower than the 270 pC/N for the BaTiO<sub>3</sub>-4 mol% LiF. Therefore, there must be something else contributing to the enhancement of their piezoelectric properties. Since the crystallographic structure of the BaTiO<sub>3</sub>-4 mol% LiF

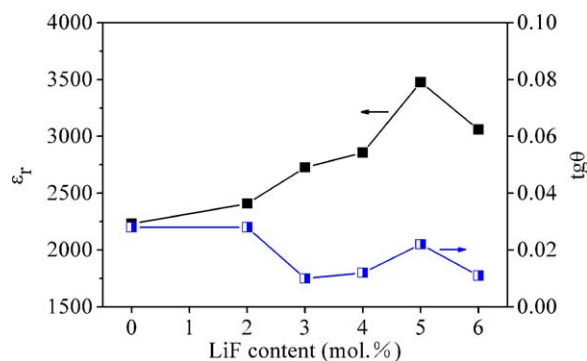


Fig. 6. Dielectric properties at 1 kHz of BaTiO<sub>3</sub>-xLiF ceramics sintered at 1100 °C as a function of LiF content.

is closer to the transition between tetragonal and orthorhombic symmetry as compared with those of the 5–6 mol% LiF added samples (Fig. 4), the change of crystallographic structure may provide a favorable condition for easier motion of domains. In other words, the  $d_{33}$  value is principally determined by crystallographic structure rather than grain size if the sample has the same high density.

Fig. 6 shows the dielectric constant ( $\epsilon_r$ ) and dielectric loss ( $\tan\delta$ ) at 1 kHz for BaTiO<sub>3</sub>-xLiF ceramics sintered at 1100 °C as a function of LiF content. Because of low relative density (<85%), the  $\epsilon_r$  value of pure BaTiO<sub>3</sub> ceramic is 2231, and increases continually to a peak value of  $\epsilon_r$  = 3500 as  $x$  = 5 mol%. The reason for this is that the increased density is favorable for enhancing dielectric property.<sup>14,15</sup> The pure BaTiO<sub>3</sub> ceramics show the highest  $\tan\delta$  = 0.028, which decreases to 0.01 as 3 mol% LiF is added. The variation in  $\tan\delta$  is similar to that in  $\epsilon_r$  for the samples with 3–6 mol% LiF and is opposite to that in  $\epsilon_r$  for the samples with 0–3 mol% LiF.

Fig. 7 shows the frequency dependence of the dielectric constant ( $\epsilon_r$ ) for BaTiO<sub>3</sub>-xLiF ceramics sintered at 1100 °C. The  $\epsilon_r$  for BaTiO<sub>3</sub>-xLiF ceramics ( $x$  = 0–6 mol%) changes slightly with raising measuring frequencies from 100 Hz to 1 MHz, while the  $\epsilon_r$  is unstable at high frequencies for the samples with  $x$  = 3–6 mol%. It has been reported that the  $\epsilon_r$  of (Ba<sub>0.95</sub>Ca<sub>0.05</sub>)(Ti<sub>0.88</sub>Zr<sub>0.12</sub>)O<sub>3</sub> ceramics decreases as the frequency increases.<sup>16</sup> This is due to some relaxation polarization

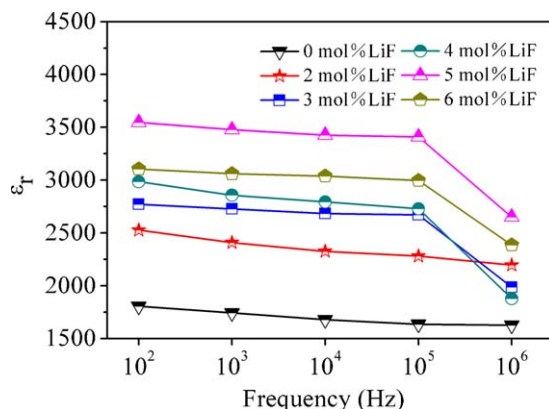


Fig. 7. Frequency dependence of  $\epsilon_r$  for BaTiO<sub>3</sub>-xLiF ceramics sintered at 1100 °C from 100 Hz to 1 MHz.

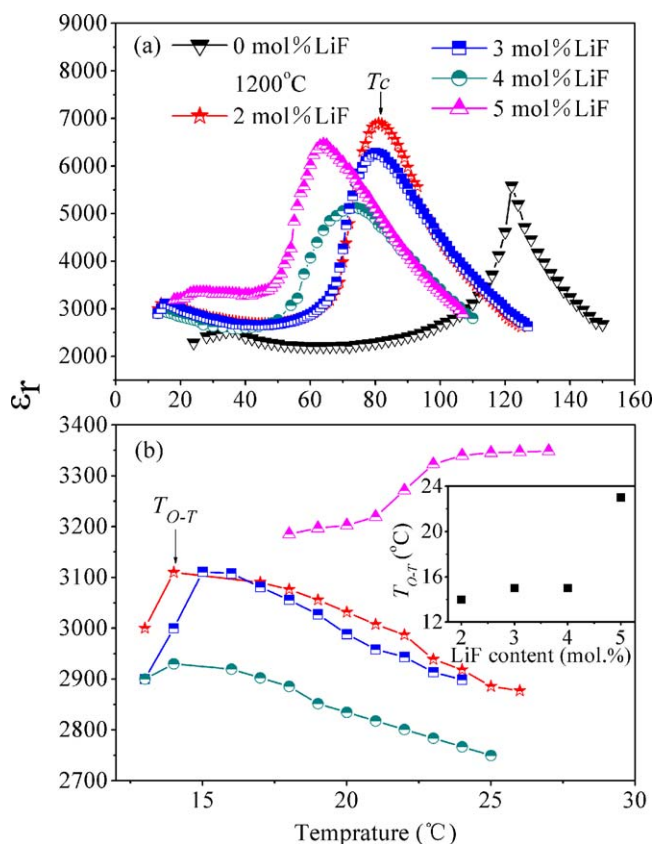


Fig. 8. Temperature dependence of  $\epsilon_r$  for BaTiO<sub>3</sub>-xLiF ceramics measured at 1 kHz between 13–150 °C (a) and 13–28 °C (b).

mechanisms at high frequencies, in which the electric charge carriers in the sample cannot respond to the rapid change in exterior electric fields when the applied electric fields exceed a certain frequency.<sup>17</sup>

Fig. 8 shows the temperature dependence of  $\epsilon_r$  for BaTiO<sub>3</sub>-xLiF ceramics measured at 1 kHz between 13 and 150 °C. As shown in Fig. 8(a), the Curie temperature ( $T_c$ ) shifts to a lower temperature as  $x$  is increased. The structure distortion produced by the substitution of Li<sup>+</sup> for Ti<sup>4+</sup> may be responsible for this kind of dielectric behavior.<sup>18</sup> On the other hand, both pure BaTiO<sub>3</sub> sintered at 1200 °C and LiF-added BaTiO<sub>3</sub> ceramics sintered at 1100 °C show an orthorhombic symmetry at room temperature (Fig. 4), so an orthorhombic–tetragonal phase transition temperature ( $T_{O-T}$ ) can be observed in Fig. 8(b). The variation in the relationship between  $T_{O-T}$  and LiF content is shown in the inset of Fig. 8(b). The  $T_{O-T}$  of BaTiO<sub>3</sub>-xLiF increases as  $x$  rises, suggesting that the crystallographic structure gradually approaches the orthorhombic symmetry. The measured  $T_{O-T}$  temperatures are lower than room temperature. However, this may be attributable to testing error.

Fig. 9 shows the polarization–electric field ( $P$ – $E$ ) hysteresis loops of BaTiO<sub>3</sub>-xLiF ceramics measured at room temperature at 100 Hz. All samples possess a typical ferroelectric polarization hysteresis loop. The inset in Fig. 9 illustrates the variation of the remanent polarization  $P_r$  and coercive field  $E_c$  of BaTiO<sub>3</sub>-xLiF ceramics as  $x$  is increased. The  $P_r$  for the LiF added ceramics reduces as compared to that for pure

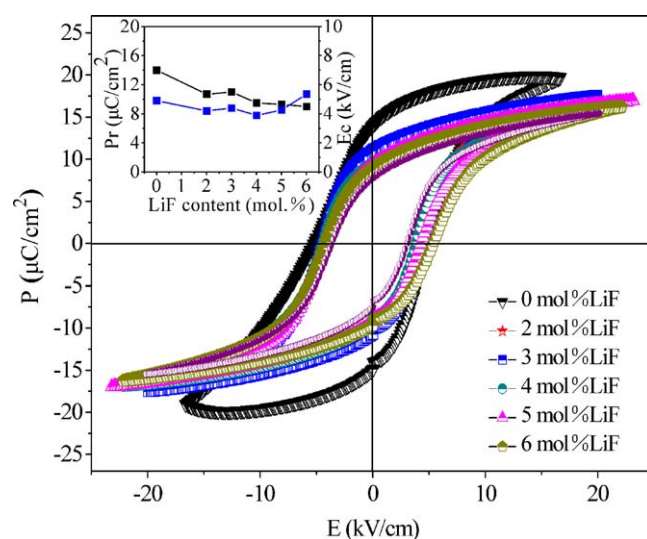


Fig. 9. Polarization–electric field ( $P$ – $E$ ) hysteresis loops of BaTiO<sub>3</sub>-xLiF ceramics measured at room temperature at 100 Hz.

BaTiO<sub>3</sub>, while  $E_c$  increases at  $x=6$  mol% in comparison with pure BaTiO<sub>3</sub>. This may be attributed to the pinning effect of domain walls caused by the increase of oxygen vacancies generated by the substitution of Li<sup>+</sup> for Ti<sup>4+</sup>.<sup>19,20</sup> Fig. 9 also shows that the leak current for the LiF added samples is lower than that for pure BaTiO<sub>3</sub> because of their better dielectric properties at room temperature.

#### 4. Conclusions

The effects of LiF content ( $x$ ) and sintering temperature on the density, phase structure and electrical properties of BaTiO<sub>3</sub>-xLiF ceramics were investigated. The densification sintering temperature of BaTiO<sub>3</sub> ceramic was reduced by approximately 250 °C after adding 6 mol% LiF. BaTiO<sub>3</sub>-4 mol% LiF ceramic sintered at 1100 °C exhibited excellent electrical properties:  $d_{33}=270$  pC/N,  $\epsilon_r=2857$ ,  $\tan\delta=0.012$ ,  $E_c=3.89$  kV/cm,  $P_r=9.5$   $\mu$ C/cm<sup>2</sup>, because it was near the phase transition boundary between tetragonal and orthorhombic symmetry in addition to its high density. BaTiO<sub>3</sub>-xLiF ceramics sintered at low temperatures with excellent electrical properties should be considered as promising lead-free piezoceramics.

#### Acknowledgments

This work was supported by Specialized Research Fund for the Doctoral Program of Higher Education (Grant No. 20090006110010) and Beijing Natural Science Foundation (Grant No. 2112028).

#### References

1. Takahashi H, Numamoto Y, Tani J, Tsurekawa S. Piezoelectric properties of BaTiO<sub>3</sub> ceramics with high performance fabricated by microwave sintering. *Jpn J Appl Phys* 2006;**45**(9B):7405–8.

2. Karaki T, Yan K, Miyamoto T, Adachi M. Lead-free piezoelectric ceramics with large dielectric and piezoelectric constants manufactured from BaTiO<sub>3</sub> nano-powder. *Jpn J Appl Phys* 2007;**46**(4):L97–8.
3. Wada S, Takeda K, Muraishi T, Kakemoto H, Tsurumi T, Kimura T. Preparation of [1 1 0] grain oriented barium titanate ceramics by template grain growth method and their piezoelectric properties. *Jpn J Appl Phys* 2007;**46**(10B):7039–43.
4. Shao SF, Zhang JL, Zhang Z, Zheng P, Zhao ML, Li JC, et al. High piezoelectric properties and domain configuration in BaTiO<sub>3</sub> ceramics obtained through the solid-state reaction route. *J Phys D: Appl Phys* 2008;**41**:125408, 5 pp.
5. Naghib-Zadeh H, Glitzky C, Oesterle W, Rabe T. Low temperature sintering of barium titanate based ceramics with high dielectric constant for LTCC applications. *J Eur Ceram Soc* 2011;**31**:589–96.
6. Caballero AC, Fernandez JF, Moure C, Duran P. ZnO-doped BaTiO<sub>3</sub>: microstructure and electrical properties. *J Eur Ceram Soc* 1977;**17**:513–23.
7. Naghib-Zadeh H, Glitzky C, Dörfel I, Rabe T. Low temperature sintering of barium titanate ceramics assisted by addition of lithium fluoride-containing sintering additives. *J Eur Ceram Soc* 2010;**30**:81–6.
8. Horchidan N, Ianculescu AC, Curecheriu LP, Tudorache F, Musteata V, Stoleriu S, et al. Preparation and characterization of barium titanate stannate solid solutions. *J Alloys Compd* 2011;**509**:4731–7.
9. Marder R, Chaim R, Chevallier G, Estournes C. Effect of 1 wt% LiF additive on the densification of nanocrystalline Y<sub>2</sub>O<sub>3</sub> ceramics by spark plasma sintering. *J Eur Ceram Soc* 2011;**31**:1057–66.
10. Akishige Y, Hiraki Y, Tsukada S, Xu J, Morito S, Ohba T, et al. Dielectric and piezoelectric properties of 10% KF-doped BaTiO<sub>3</sub> ceramics. *Jpn J Appl Phys* 2010;**49**:081501.
11. Taïbi-Benziada L, Hilal HS, Mühl R. Low temperature sintering and dielectric properties of (Ba,Ca)(Ti,Li)(O,F)<sub>3</sub> ceramics with high permittivity. *Solid State Sci* 2006;**8**:922–6.
12. Lei N, Zhu MK, Yang P, Wang LF, Hou YD, Yan H. Effect of lattice occupation behavior of Li<sup>+</sup> cations on microstructure and electrical properties of (Bi<sub>1/2</sub>Na<sub>1/2</sub>)TiO<sub>3</sub>-based lead-free piezoceramics. *J Appl Phys* 2011;**109**:054102.
13. Shen ZY, Li JF. Enhancement of piezoelectric constant  $d_{33}$  in BaTiO<sub>3</sub> ceramics due to nano-domain structure. *J Ceram Soc Jpn* 2010;**118**(10):940–3.
14. Chang YF, Yang ZP, Wei LL. Microstructure, density, and dielectric properties of lead-free (K<sub>0.44</sub>Na<sub>0.52</sub>Li<sub>0.04</sub>)(Nb<sub>0.96-x</sub>Ta<sub>x</sub>Sb<sub>0.04</sub>)O<sub>3</sub> piezoelectric ceramics. *J Am Ceram Soc* 2007;**90**(5):1656–8.
15. Zhang HL, Li JF, Zhang BP. Microstructure and electrical properties of porous PZT ceramics derived from different pore-forming agents. *Acta Mater* 2007;**55**:171–81.
16. Zhang SW, Zhang HL, Zhang BP, Zhao GL. Dielectric and piezoelectric properties of (Ba<sub>0.95</sub>Ca<sub>0.05</sub>)(Ti<sub>0.88</sub>Zr<sub>0.12</sub>)O<sub>3</sub> ceramics sintered in a protective atmosphere. *J Eur Ceram Soc* 2009;**29**:3235–42.
17. Du HL, Yao X. Effects of Sr substitution on dielectric characteristics in Bi<sub>1.5</sub>ZnNb<sub>1.5</sub>O<sub>7</sub> ceramics. *Mater Sci Eng B* 2003;**99**:437–40.
18. Bhaskar Reddy S, Prasad Rao K, Ramachandra Rao MS. Effect of La substitution on the structural and dielectric properties of BaZr<sub>0.1</sub>Ti<sub>0.9</sub>O<sub>3</sub> ceramics. *J Alloys Compd* 2009;**481**:692–6.
19. Lin DM, Kwok KW, Chan HL. Effects of MnO<sub>2</sub> on the microstructure and electrical properties of 0.94(K<sub>0.5</sub>Na<sub>0.5</sub>)NbO<sub>3</sub>–0.06Ba(Zr<sub>0.05</sub>Ti<sub>0.95</sub>)O<sub>3</sub> lead-free ceramics. *Mater Chem Phys* 2008;**109**(2–3):p.455.
20. Zuo RZ, Ye C, Fang XS. Processing and piezoelectric properties of (Na<sub>0.5</sub>K<sub>0.5</sub>)<sub>0.96</sub>Li<sub>0.04</sub>(Ta<sub>0.1</sub>Nb<sub>0.9</sub>)<sub>1-x</sub>Cu<sub>x</sub>O<sub>3-3x/2</sub> lead-free ceramics. *J Am Ceram Soc* 2008;**91**(3):p.914.